DOI: https://doi.org/10.36094/sc.v89.2023.Time-delayed_Feedback_Control_of_Spatiotemporal.Paul.406

ARTICLE

Sci. and Cult. 89 (11–12) : 406-410 (2023)

TIME-DELAYED FEEDBACK CONTROL OF SPATIOTEMPORAL DYNAMICS IN A NETWORK OF DIGITAL PHASE-LOCKED LOOPS

BISHWAJIT PAUL*

Digital phase-locked loops (DPLLs) are unavoidable electronic system in modern network communication. They are nonlinear in characteristics; therefore, the collective dynamics of those systems are extremely complex. This paper explores that; time-delayed feedback control algorithm is able to control unstable spatiotemporal dynamics that appear in a one dimensional network of locally coupled DPLLs. Such network shows several unstable spatiotemporal patterns; like, frozen random pattern, pattern selection, spatiotemporal intermittency and spatiotemporal chaos. It is explored that, proper feedback control parameter is able to control unstable dynamics into synchronised dynamics. Analytical stability condition for the controlled network is also derived.

Introduction

Digital phase-locked loops (DPLLs) are the basic components of electronic-communication systems and networking. They are also widely used in electronic control systems, computers, memory systems, etc. In all those systems, phase-locking is most important requisite. This can be achieved by using wide variety of phase-locked loops. Important examples of DPLLs are; uniform sampling DPLL[1], positive zero-crossing DPLL (ZC1-DPLL)[2-4], dual-sampler based zero-crossing DPLL[5], digital tan-lock loop[6], bang-bang DPLL[7], etc. All these are nonlinear in characteristics and exhibit chaotic dynamics. Among all of them, ZC1-DPLL is most widely used in engineering systems due to hardware simplicity and reliability.

Initially, DPLLs ware used as isolated system; like motor speed control, coherent phase detection in radio receiver, frequency modulation and synthesis, etc. But with the advent of new technology, they are now a days widely used in networks; e.g., in synchronous communication systems, internet, FPGA systems, etc. So, investigation on the collective behaviour of DPLLs is very important from application point of view. Previously, the collective dynamics of ZC1-DPLLs are studied under local[8] and non-local coupling[9]. Such networks exhibit several unstable spatiotemporal patterns; namely, frozen random pattern (FRP), pattern selection (PS), spatiotemporal intermittency (STI), spatiotemporal chaos (STC), etc. Such instabilities appear for large available parameter values of the network. But in real engineering applications such unstable dynamics makes the systems unreliable. In most of the applications, synchronization in the network is the utmost criteria. So stabilization of unstable dynamics into stable synchronized dynamics is very essential for reliable network operations.

Stabilization of uncontrolled dynamics and chaos is always challenging to researchers. There are varieties of control methods to stabilize chaotic systems. Some examples are; OGY[10], TDFC[11], pinning, robust control algorithms, etc. They can control isolated nonlinear systems well. For space extended coupled nonlinear systems, all control methods are not suitable. TDFC and pinning control methods are suitable for controlling complex network systems. But, applying pinning control method in the engineering networks is challenging due to difficulty in finding proper pinning nodes. In this paper,

* *Department of Physics, Krishnagar Government College, Krishnagar-741 101, West Bengal, India.
e-mail: paulbishwajit10@gmail.com

we apply time-delayed feedback control (TDFC) algorithm to control instability in a one dimensional (1D) network of locally coupled ZC1-DPLLs. Firstly, we map all the spatiotemporal patterns of the controlled network in a phase diagram. Proper choice of the delayed feedback strength can control considerable uncontrolled region of the phase diagram. Then we explore that; TDFC algorithm can control FRP, PS, STI and even STC. We also analytically determine the condition of stable synchronization in the network and identify the zone of stable phase locked operation in the parameter space. It is found that, the analytical results fairly agree with the numerical results.

An isolated ZC1-DPLL and its one-dimensional Network with Local Coupling

Fig. 1(a) shows the operational loop diagram of a ZC1-DPLL. It comprises of a sample and hold unit (S/H), a digital filter (DF) and a digital controlled oscillator (DCO). Let, noise free incoming signal $s(t) = a\sin(\omega t + \theta)$ is sampled at its positive zero crossing edges by the S/H that produces sampled signal χ_k at time instant $t_k\,[k \in 0,1,2,...]$. Where a, ω and θ are respectively the amplitude, angular frequency and initial phase. The t_k is determined by the DCO controlled by c_k obtained by digital filtering of χ_k. In this way, phase locking is achieved by self feedback control of DCO frequency.

If ω_0 be free-running angular frequency of the DCO, then the input signal can be written as $s(t) = a\sin\phi(t)$. Where, $\phi(t) = \omega_0 t + \psi(t)$ and $\psi(t) = (\omega - \omega_0)t + \theta$. So, χ_k at t_k is $\chi_k = s(t_k) = a\sin(\phi_k)$. Now, $\phi_k = \phi(t_k) = \omega_0 t_k + \psi_k$. The control signal is $c_k = G_0\chi_k$, where G_0 is gain of the DF. Instantaneous DCO time period T_k is logically $T_k = t_k - t_{k-1}$. The algorithm for the next time period of DCO is $T_{k+1} = T_0 - c_k$[4]; where, $T_0 = 2\pi/\omega_0$. Now considering $t_0 = 0$, the successive sampling instants are, $t_k = kT_0 - \sum_{i=0}^{k-1} c_i$. So, the phase error at t_k becomes $\phi_k = \psi_k - \omega_0\sum_{i=0}^{k-1} c_i$. Phase difference between successive instants is, $\phi_{k+1} - \phi_k = \Lambda - \xi\omega_0 G_0\chi_k$; with $\xi = \omega/\omega_0$ and $\Lambda = 2\pi(\xi - 1)$ are constants. Therefore, the phase error equation of the isolated ZC1-DPLL becomes[3],

$$\phi_{k+1} = \Lambda + \phi_k - \xi K_1 \sin(\phi_k). \tag{1}$$

Where, $K_1 = a\,\omega_0 G_0$ is called loop gain of the ZC1-DPLL. All ϕ_k are bounded in $[-\pi : +\pi]$.

Fig. 1(b) shows the ring network topology with periodic boundary condition. It consists of *N* identical ZC1-DPLLs shown with solid circles (indexed by $i \in 1,2,3\,...\,N$) with local coupling. Fig. 1(c) shows practical realization of the coupling scheme for the *i*-th ZC1-DPLL (considering $\gamma = 0$; i.e., discarding the dotted-lined block). Here, ε is the coupling strength. So, the signal z_k^i becomes $z_k^i = \chi_k^i + \frac{\varepsilon}{2}\left(\chi_k^{i-1} + \chi_k^{i+1}\right)$. Here, χ_k^{i-1} and χ_k^{i+1} are respectively from (*i* – 1) and (*i* + 1)-th nodes. Now employing same logic as that of an isolated ZC1-DPLL, the phase error equation of the network (uncontrolled) becomes[9],

$$\phi_{k+1}^i = \Lambda + \phi_k^i - \xi K_1 \sin\left(\phi_k^i\right) - \frac{\varepsilon}{2}\xi K_1\left[\sin\left(\phi_k^{i-1}\right) + \sin\left(\phi_k^{i+1}\right)\right]. \tag{2}$$

Implementation of TDFC algorithm on the network of ZC1-DPLLs

TDFC algorithm is shown in Fig. 1(c) with a dotted box.

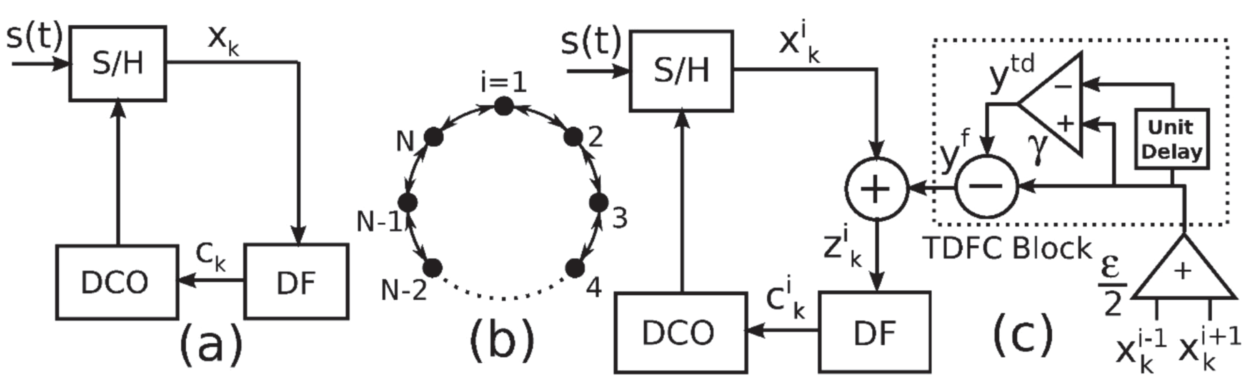

Fig. 1. (a) Functional loop diagram of an isolated ZC1-DPLL. (b) Coupling topology of one dimensional ring network of ZC1-DPLLs with local coupling. (c) Practical realization of ring network for the i-th ZC1-DPLL (neglecting dotted box, i.e., setting γ = 0) and the dotted box shows the realization of TDFC.

It uses one unit delay block and a difference amplifier with controllable gain parameter γ. It produces a time-delayed difference signal $y^{td} = \gamma \frac{\varepsilon}{2}\left(\chi_k^{i-1} + \chi_k^{i+1} - \chi_{k-1}^{i-1} - \chi_{k-1}^{i+1}\right)$, that is subtracted from $\frac{\varepsilon}{2}\left(\chi_k^{i-1} + \chi_k^{i+1}\right)$ to get y^f. Therefore, $z_k^i = \chi_k^i + y^f = \chi_k^i + \frac{\varepsilon}{2}\left(\chi_k^{i-1} + \chi_k^{i+1}\right) - \gamma \frac{\varepsilon}{2}\left(\chi_k^{i-1} - \chi_{k-1}^{i-1} + \chi_k^{i+1} - \chi_{k-1}^{i+1}\right)$. Now, using the logic as before, the system equation for the controlled 1D network becomes,

$$\phi_{k+1}^i = \Lambda + \phi_k^i - \xi K_1 \sin\left(\phi_k^i\right) - \frac{\varepsilon}{2}\xi K_1\left[\sin\left(\phi_k^{i-1}\right) + \sin\left(\phi_k^{i+1}\right)\right]$$

$$+\gamma \frac{\varepsilon}{2}\xi K_1\left[\sin\left(\phi_k^{i-1}\right) - \sin\left(\phi_{k-1}^{i-1}\right) + \sin\left(\phi_k^{i+1}\right) - \sin\left(\phi_{k-1}^{i+1}\right)\right]. \tag{3}$$

Here, γ is called feedback control parameter. This system equation is equivalent to N coupled difference equations. If we set $\gamma = 0$, the Eq. (3) reduced to uncontrolled network [Eq. (2)]. Again if we put $\varepsilon = 0$, then it converts into N uncoupled ZC1-DPLLs.

Stability Analysis of the Controlled Network

Steady state phase error ϕ_s of the network [Eq. (3)] is given by $\phi_s = \sin^{-1}\left(\frac{\Lambda}{\xi K_1(1+\varepsilon)}\right)$. Linear stability of the network at ϕ_s can be derived by diagonalizing the Jacobi matrix of the system equation. The system Eq. (3) can be represented in terms of a ($2N \times 2N$) Jacobi matrix as: $J_{2N} = \begin{pmatrix} A_N & B_N \\ 0_N & I_N \end{pmatrix}$. Where; 0_N, I_N are respectively null matrix and identity matrix of order ($N \times N$) each. A_N and B_N are ($N \times N$) circulant matrices of the following forms:

$$A_N = \begin{pmatrix} A_d & A_r & 0 & 0 & \cdots & A_l \\ A_l & A_d & A_r & 0 & \cdots & 0 \\ 0 & A_l & A_d & A_r & \cdots & 0 \\ \vdots & \vdots & \vdots & \vdots & \vdots & \vdots \\ A_r & 0 & 0 & \cdots & A_l & A_d \end{pmatrix},$$

$$B_N = -\gamma \frac{\varepsilon}{2} K_1 \xi \begin{pmatrix} 0 & 1 & 0 & 0 & \cdots & 1 \\ 1 & 0 & 1 & 0 & \cdots & 0 \\ 0 & 1 & 0 & 1 & \cdots & 0 \\ \vdots & \vdots & \vdots & \vdots & \vdots & \vdots \\ 1 & 0 & 0 & \cdots & 1 & 0 \end{pmatrix}. \tag{4}$$

Where, $A_d = 1 - \xi K_1 \cos(\phi_s)$, $A_l = A_r = \frac{\varepsilon}{2}\xi K_1 (\gamma - 1)\cos(\phi_s)$. Basically, J_{2N} is a block circulant matrix. A circulant matrix is diagonalizable by a Fourier matrix[12]. The stability condition of Eq. (3) can be obtained by finding eigenvalues of J_{2N} and using the condition: absolute of real parts of all the eigenvalues should be less than one. Now $2N$ eigenvalues are given by, $\lambda_l = \frac{1}{2}\left\{a_d(l) \pm \sqrt{a_d^2(l) - \gamma\varepsilon\xi K_1 \cos\left(\frac{2\pi l}{N}\right)}\right\}$; where, $a_d(l) = A_d + 2A_l \cos\left(\frac{2\pi l}{N}\right)$, with $l \in (1, 2, 3, \ldots N)$. Now, the stability condition at steady state reduces to $\left|\mathrm{Re}(\lambda_l)\right|_{\max} < 1$. Analytical stability zones of the controlled network are shown in Fig. 2.

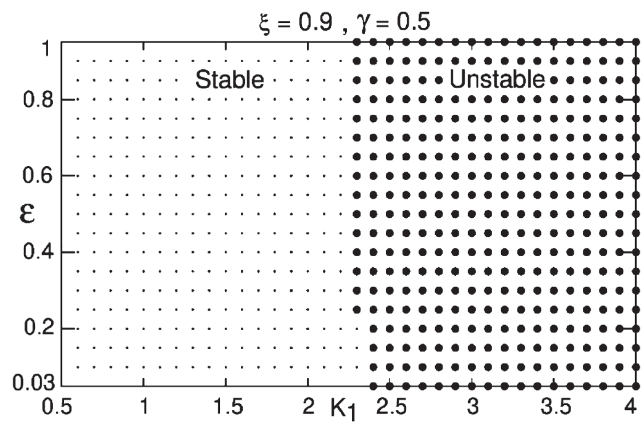

Fig. 2. Analytical stable and unstable zones of the network in $K_1 - \varepsilon$ space for $\gamma = 0.5$.

Numerical Results

Numerical studies on the system Eq. (2) explore diverse spatiotemporal patterns. Throughout the simulation, we keep $N = 256$ and used random initial condition generated uniformly within $[-\pi : +\pi]$. We permit input signal to a wide range of frequency offset such that $\xi = 0.9$. Throughout the study, first 10000 iterations are neglected to eliminate transients.

Dynamics of uncontrolled network : The network exhibits several spatiotemporal patterns. They are mapped with distinct points on a phase diagram ($K_1 - \varepsilon$ space) shown in Fig. 3(a). The thick dashed line represents analytically obtained boundary for SFP. Fig. 3(b)-(f) show space-time plot of ϕ_k^i with lines for different dynamical patterns. As K_1 increases, for constant ε, network shows

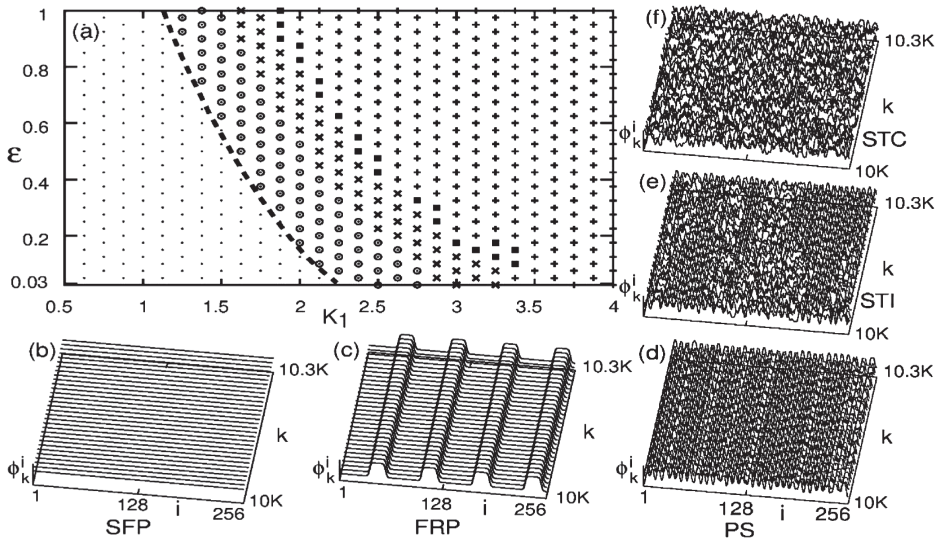

Fig. 3. (a) Phase diagram of uncontrolled network ($\xi = 0.9$). Points specification: (1) dots: SFP, (2) doted circles: FRP, (3) crosses: PS, (4) filled squares: STI, (5) plus signs: STC. (b)-(f) space-time plots of ϕ_k^i for constant $\varepsilon = 0.5$. (b) K_1 = 1.5 (c) K_1 = 1.7 (d) K_1 = 2.3 (e) K_1 = 2.38 (f) K_1 = 2.6.

phase transition from stable state (SFP) to complete chaotic state (STC) via FRP, PS and STI.

Fig. 3(b) shows SFP (for smaller K_1); where the network maintain a constant phase $\left(\phi_s\right)$ spatially as well as temporally. Therefore, the network becomes completely synchronized. Fig. 3(c) shows FRP; where the network is divided into domains of random size. As K_1 is increased, the domains become very small and almost equal in size; it is called PS [Fig. 3(d)]. Fig. 3(e) shows STI; where space-time region looks like a mixture of regular and chaotic dynamics. Finally, for even larger values of K_1, the network becomes completely chaotic [Fig. 3(f)].

Control of unstable dynamics using TDFC : Fig. 4(a) shows the controlled dynamics in similar parameter space for γ = 0.5. It is obvious that, a considerable portion of unstable regions become controllable with the application of TDFC. The region of SFP matches with the analytical result [see Fig. 2]. It is found that, proper choice of control parameter can stabilize some FRP, PS, STI and STC regions of the uncontrolled network. Fig. 4(b1) shows that, for K_1 = 2.1 and ε = 0.3, the uncontrolled network shows FRP. With the application of TDFC with γ = 0.44, the dynamics transformed into SFP shown in Fig. 4(b2). Similarly, PS [Fig. 4(c1)] in the original network (with K_1 = 2.05 and ε = 0.7) become synchronized with a control strength γ = 0.47. Fig. 4(d1) and (e1) show STI and STC for the uncontrolled network with parameters K_1 = 2.22, ε = 0.6 and K_1 = 2.20, ε = 0.9, respectively. Such chaotic dynamics are also controllable with TDFC. Fig. 4 (d2) and (e2) shows the controlled SFP from STI and STC respectively. It is also noted that, choice of γ is not limited to a narrow range. Instead the network remains synchronized for wide range of γ values (typically, $\Delta\gamma \approx 0.1$).

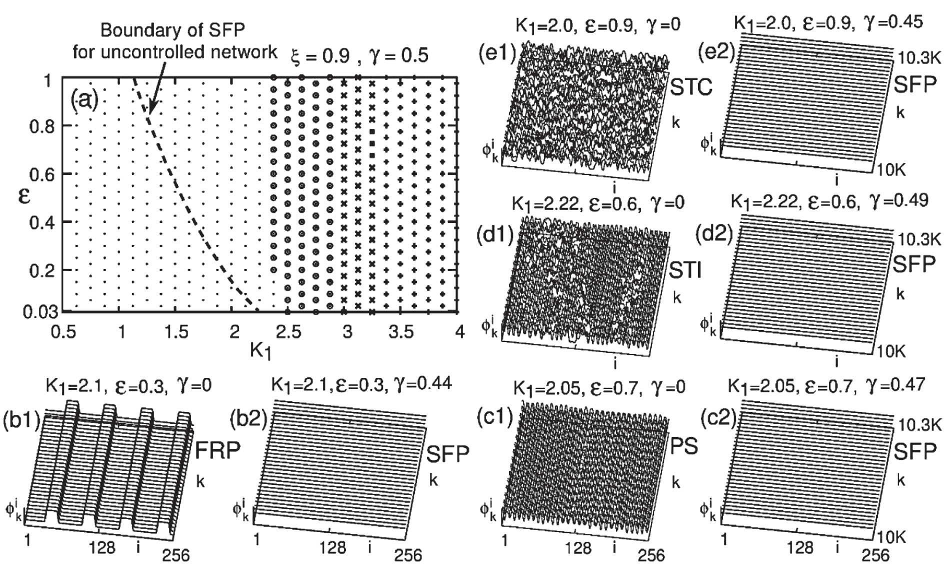

Fig. 4. (a) Phase diagram of controlled network (γ = 0.5). Stabilization of network dynamics on TDFC: (b1)-(b2) FRP to SFP, (c1)-(c2) PS to SFP, (d1)-(d2) STI to SFP, (e1)-(e2) STC to SFP.

Conclusion

We have shown that, TDFC algorithm can effectively control all types of unstable spatiotemporal dynamics including spatiotemporal chaos in a network of ZC1-DPLL. Proper choice of control parameter can stabilize wide region of parameter space. This control method does not affect steady state phase error of the original network (ϕ_s is independent of γ). TDFC can control STC that appears for larger values of ε in parameter space. So, larger ε corresponds to lesser steady state phase error; this leads to better synchronization in the network. We hope, this study will help engineers in improving their network stability and reliability. ❐

References

1. M. Zoltowski, *Signal Processing*, Vol. **81**, 735-789 (2001).
2. G. Bernstein, M. Liberman and A. Lichtenberg, *IEEE Trans. Commun.*, **37**(10), 1062-1070(1989).
3. G.A. Leonov and S. M. Seledzhi, *Int. J. Bifurcation and Chaos*, **15**, 1347-1360 (2005),
4. T. Banerjee and B.C. Sarkar, *Int. J. Bifurcation and chaos*, **22**, 1230044 (2012).
5. T. Banerjee and B.C. Sarkar, *Int. J. Electron.*, **96**, 717-732(2009).
6. J. Lee and C. Un, *IEEE Trans. Commun.* **30**, 2398-2411(1982).
7. N.D. Dalt, *IEEE Trans. on Circuit and Syst.-I*, **52**, 21-31(2005).
8. T. Banerjee, B. Paul and B.C. Sarkar, *Chaos*, **24**(1), 013116(2014).
9. B. Paul and T. Banerjee, *Chaos*, **29**(1), 013102 (2019).
10. E. Ott, C. Grebogi and J.A. Yorke, *Phys. Rev. Lett.,* **64** (11), 1196-1199 (1990).
11. K. Pyragas, *Phys Lett. A,* **170**, 42-428 (1992).
12. P.M. Gade, *Phys. Rev. E.*, **57**(6), 7309-7312 (1998).